Analytical and Bioanalytical Chemistry
https://doi.org/10.1007/s00216-018-1454-3

RESEARCH PAPER

Application of central composite design for the optimization of electrode surface composition for glucose biosensor fabrication

İrem Okman Koçoğlu[1] · Pınar Esra Erden[1,2] · Adnan Kenar[1] · Esma Kılıç[1]

Received: 16 October 2018 / Accepted: 24 October 2018

Abstract

The use of a central composite design (CCD) for the optimization of electrode surface composition and its application to develop an amperometric glucose biosensor as a model system are described. A five-level three-factorial CCD was applied to determine the optimum electrode surface composition for three critical variables: amounts of carboxylated multiwall carbon nanotubes (c-MWCNT), titanium dioxide nanoparticles (TiO_2NP), and glucose oxidase (GOx). The statistical significance of the model and factors were evaluated using the variance analysis (ANOVA) at 95% of confidence level. The optimized electrode surface composition was used for the fabrication of the glucose biosensor. The resulting biosensor showed linear response to glucose from 2.0×10^{-5} to 1.9×10^{-3} M with a detection limit of 2.1×10^{-6} M and sensitivity of 168.5 μA mM^{-1} cm^{-2} under optimal experimental conditions. Analytical performance parameters of the biosensor were also compared with those obtained with the glucose biosensors fabricated using the electrode compositions optimized by conventional one factor-at-a-time method and 2^2 CCD (for c-MWCNT and TiO_2NP amounts). The optimization of the critical variables, achieved by CDD, leads us to fabricate the glucose biosensor in the best electrode surface composition which was promoted by the improved analytical performance. The proposed biosensor was applied to the analysis of glucose in serum samples and the obtained results were well correlated with the results of reference method.

Keywords Glucose biosensor · Titanium dioxide nanoparticles · Carbon nanotube · Central composite design

Introduction

Electrochemical enzyme electrodes are one of the most important types of biosensors due to their high specificity, short time of analyses, and good selectivity [1–3]. Currently improving the sensing performance of electrochemical biosensors continues to be the primary focus of biosensor research [4]. Recent developments in nanomaterials have greatly enhanced the sensitivity and selectivity of electrochemical biosensors [4, 5]. Carbon-based nanomaterials, especially carbon nanotubes (CNTs), are extremely attractive for biosensor design as they can combine properties of the large surface area, excellent electron conductance, acceptable biocompatibility, chemical and electrochemical stability, and high mechanical resistance [6]. Since metal oxide nanoparticles (MONPs) possess unique features such as large surface-to-volume ratio, high surface reaction activity, and high catalytic efficiency, so far increasing number of studies have been reported on the use of novel CNTs–MONPs nanocomposites for biosensor applications [7–10]. Various MONPs such as SnO_2, Fe_3O_4, Co_3O_4, ZnO, Bi_2O_3, and TiO_2 have been used to prepare CNTs–MONPs nanocomposites [10–15]. These nanocomposites were reported to improve the analytical performance of the biosensors. TiO_2 is a very attractive semiconductor material which has found application in different areas including solar cells, photocatalysts, cosmetics, batteries, and biomaterials [16]. On the other hand, TiO_2 nanoparticles have gained increasing attention in the field of biosensors due to their special properties such as porous structure, chemical stability, large specific surface area, excellent biocompatibility, photocatalytic

Electronic supplementary material The online version of this article (https://doi.org/10.1007/s00216-018-1454-3) contains supplementary material, which is available to authorized users.

✉ Esma Kılıç
ekilic@science.ankara.edu.tr

[1] Department of Chemistry, Faculty of Science, Ankara University, Tandoğan, 06100 Ankara, Turkey

[2] Department of Chemistry, Polatlı Faculty of Science and Arts, Ankara Hacı Bayram Veli University, Polatlı, 06900 Ankara, Turkey

Published online: 22 November 2018

activity, and photosensitivity [17, 18]. Various biosensors based on TiO_2 nanomaterials have been reported [19–24].

The optimization of electrode surface composition is a crucial step in the fabrication of modified enzyme based- biosensors. Therefore, the effects of the modification materials and their synergistic interactions must be evaluated. Experimental designs can be used to investigate and optimize the influence of the important variables in a method to enhance the performance and decrease the number of experiments [25]. Among different experimental designs, central composite design (CCD) which is a combination of mathematical and statistical method is widely applied for the determination of the significant variables and optimum conditions [26–29]. In comparison with the laborious and time-consuming conventional one factor-at-a-time method, optimization by CCD approach can be useful for the rapid gathering of experimental research results [30]. In biosensor research, CCD is mainly used for the optimization of experimental variables such as temperature, pH and applied potential [31–35]. To the best of our knowledge, the use of CCD for the optimization of electrode surface composition is not a common approach in biosensor fabrication and a limited number of studies have been reported [27, 36–38]. The use of CCD approach in the construction and characterization of an amperometric biosensor has the following advantages: (i) more information can be obtained with minimum number of experiments with consequent savings in the time and costs that are usually involved in optimization procedures; (ii) optimum experimental conditions or electrode composition can be determined resulting in improved response and sensitivity; (iii) this approach allows to determine individual, interactive, and quadratic effects of optimization parameters on the biosensor response.

Electrochemical biosensors have been successfully used for the quantification of blood glucose which is a clinically important parameter for diabetic health care, diagnosis, and treatment [39, 40]. The purpose of this study is to determine optimum amounts of c-MWCNT, TiO_2NP and GOx in the chitosan (CT) matrix by 2^3 factorial CCD and fabricate an amperometric glucose biosensor using this composition. GOx was selected as a model enzyme due to its biochemical stability, low cost, and practical use [41]. We believe that this is the first work that shows the use of CCD for the optimization of electrode surface composition to fabricate an amperometric glucose biosensor based on carbon nanotubes and titanium dioxide nanoparticles. Thus, this strategy could open new opportunities in the design and development of enzyme-based biosensors. After the optimization of electrode surface composition by CCD, the experimental variables and the analytical characteristics of the biosensor were determined and the results were compared with those obtained with the glucose biosensor constructed using the electrode composition optimized by conventional one factor-at-a-time method. The analytical applicability of the resulted biosensor for glucose analysis in serum samples was also presented.

Materials and methods

Reagents

GOx (159 units/mg solid), TiO_2NP (< 100 nm particle size), $K_3Fe(CN)_6$, $K_4Fe(CN)_6.3H_2O$, urea, sodium chloride, sodium monohydrogenphosphate, sodium dihydrogenphosphate, ascorbic acid, chitosan, Nafion® (5 wt% in lower aliphatic alcohols), and uric acid were obtained from Sigma-Aldrich (St. Louis, MO, USA). c-MWCNT (O.D. < 8 nm and length 10–30 μm) were purchased from Cheap Tubes Inc. (Brattleboro, USA). Glucose was bought from Fluka (Buchs, Switzerland).

Instrumentation

Electrochemical studies were conducted on an Iviumstat electrochemical analyzer (Ivium Technologies, Netherlands) with a three-electrode system consisting GOx/TiO_2-c-MWCNT-CT modified glassy carbon electrode (GCE) (3.0 mm diameter) utilized as working, Ag/AgCl (BAS MF 2052) as reference and Pt wire (BAS MW 1034) as auxiliary electrode. The amperometric experiments were performed at +0.70 V vs. Ag/AgCl in stirred phosphate buffer solution (PBS) (0.025 M, pH 8.0). The morphology of modified electrodes was investigated with a FEI, Quanta 450 FEG model scanning electron microscope. The energy-dispersive X-ray (EDX) spectroscopy study was performed with a Bruker detector. Electrochemical impedance spectroscopy (EIS) and cyclic voltammetry (CV) experiments were performed in 0.1 M KCl containing 5.0 mM $K_3[Fe(CN)_6]/K_4[Fe(CN)_6]$ (1:1) to investigate the electrochemical characteristics of the modified electrodes. Cyclic voltammograms were obtained within the potential range from − 0.40 to + 0.80 V at a scan rate of 50 mV s^{-1}. In EIS experiments, the alternating voltage was 10 mV and the frequency range was from 10^5 to 0.05 Hz.

Central composite design for the optimization of electrode surface composition

CCD was used to optimize the surface composition of GOx/TiO_2-c-MWCNT-CT/GCE. Three independent variables (c-MWCNT, TiO_2NP, and GOx) were used as an experimental design. Considering that the biosensor response is directly related to the c-MWCNT, TiO_2NP, and GOx amounts on the electrode surface and that synergistic effects between these variables can occur, surface composition was optimized by a 2^3 CCD. As a result, c-

MWCNT and TiO_2NP amounts (low 10 mg mL^{-1} and high 30 mg mL^{-1}) and GOx amount (low 2 U μL^{-1} and high 4 U μL^{-1}) have been considered. In this design, a total of 22 experiments were performed, including 8 factorial points, 6 axial points and 8 central points. α value was used as 1.68 for ortagonal and rotatable design. The design allowed each variable to range in five levels which are shown in Table 1. The design matrix is presented in Table 2. c-MWCNT and TiO_2NP were dispersed in CT and 6 μL of this mixture was dropped on a GCE and then 10 μL GOx was immobilized on the electrodes to fabricate the 22 modified glucose biosensors. The amperometric response currents of these biosensors, recorded for a 8.0×10^{-5} M glucose solution, was taken as response to analyze the experimental design (Table 2).

The three independent variables have mathematical relationship that can be approximated by the second order polynomial model:

$$Y = \beta_0 + \beta_1[\text{c–MWCNT}] + \beta_2[\text{TiO}_2\text{NP}] + \beta_3[\text{GOx}] + \beta_{11}[\text{c–MWCNT}]^2 + \beta_{22}[\text{TiO}_2\text{NP}]^2 + \beta_{33}[\text{GOx}]^2 + \beta_{12}[\text{c–MWCNT}]\,[\text{TiO}_2\text{NP}] + \beta_{13}[\text{c–MWCNT}]\,[\text{GOx}] + \beta_{23}\,[\text{TiO}_2\text{NP}]\,[\text{GOx}]$$

where Y is the predicted amperometric current response; β_0 is the model constant; β_1, β_2, β_3, β_{11}, β_{22}, β_{33}, β_{12}, β_{13}, and β_{23} are the coefficients found by the model, which represented the linear, quadratic and interactive effects of [c-MWCNT], [TiO_2NP] and [GOx] on the current response, respectively.

CCD was applied with the assistance of Design-Expert software package (Version 10.0.3, Stat – Ease Inc., Minneapolis, USA). The statistical significance of the model and factors were evaluated using the variance analysis (ANOVA) at 95% of confidence level ($p = 0.05$). A regression analysis and the plotting of response surface were also performed to establish an optimum surface composition for biosensor preparation.

Table 1 Experimental factors and levels in the 2^3 CCD for the optimization of c-MWCNT, TiO_2NP, and GOx amounts

Factor	Units	Level				
		− 1.68	− 1	0	1	+ 1.68
A: c-MWCNT	mg mL^{-1}	3.18	10	20	30	36.82
B: TiO_2NP	mg mL^{-1}	3.18	10	20	30	36.82
C: GOx	unit/10 μL	13.18	20	30	40	46.82

Table 2 2^3 CCD, experimental and predicted amperometric response currents obtained with GOx/TiO_2-c-MWCNT-CT/GCE in 8.0×10^{-5} M glucose solution (0.025 M PBS, pH 8)

Electrode	A	B	C	Amperometric current response, nA		
				Experimental	Predicted	Residual
1	− 1	− 1	− 1	395	470.3	− 75.3
2	1	− 1	− 1	700	663.2	36.8
3	− 1	1	− 1	594	508.8	85.2
4	1	1	− 1	1105	1018.8	86.2
5	− 1	− 1	1	626	711.8	− 85.8
6	1	− 1	1	811	895.8	− 84.8
7	− 1	1	1	555	591.4	− 36.4
8	1	1	1	1168	1092.3	75.7
9	− 1.68	0	0	268	201.0	67.0
10	1.68	0	0	717	784.5	− 67.5
11	0	− 1.68	0	802	667.4	134.6
12	0	1.68	0	750	875.1	− 125.1
13	0	0	− 1.68	820	898.8	− 78.8
14	0	0	1.68	1242	1163.7	78.3
15	0	0	0	1145	1141.2	3.8
16	0	0	0	1175	1141.2	33.8
17	0	0	0	1168	1141.2	26.8
18	0	0	0	935	1141.2	− 206.2
19	0	0	0	1171	1141.2	29.8
20	0	0	0	1180	1141.2	38.8
21	0	0	0	1202	1141.2	60.8
22	0	0	0	1154	1141.2	12.8

Biosensor preparation

After the optimization of electrode surface composition by CCD, the biosensor was prepared according to the following procedure: The bare GCE was polished with 1.0, 0.3, and 0.05 μm alumina slurry, respectively, and ultrasonically cleaned in distilled water and ethanol before the modification step. 5.0 g of chitosan was dissolved in 50.0 mL of acetate buffer by magnetic stirring and sonicated for 2 h to get a clear solution. TiO_2NP (22.2 mg) and c-MWCNT (24.1 mg) were dispersed into 1 mL of aqueous chitosan solution and this mixture was kept under mechanical stirring for 1 h and sonicated for 2 h. Six microliters of this solution was coated onto GCE surface and allowed to dry. Ten microliters of GOx solution (3.89 U μL^{-1}) was further dropped onto the modified sensing interface (TiO_2-c-MWCNT-CT/GCE) and allowed to dry at + 4 °C to fabricate the glucose biosensor. Finally, Nafion (0.25%) was pipetted on the top of the GOx/TiO_2-c-MWCNT-CT/GCE to enhance the anti-interferent ability of the biosensor and minimize the loss of the enzyme. The resulting biosensor was washed with 0.025 M PBS (pH 8.0), dried and finally stored at + 4 °C until use. The fabrication

procedure of the glucose biosensor based on GOx/TiO_2-c-MWCNT-CT modified GCE is summarized in Scheme 1.

Results and discussion

Optimization of TiO_2NP, c-MWCNT, and GOx amounts using CCD

The analytical performance of a biosensor is highly dependent on the surface composition of the modified electrode. Therefore, the amounts of the components used in surface modification need to be carefully optimized. In our study, c-MWCNT, TiO_2NP, and GOx amounts can be considered as experimental variables that directly affect the performance characteristics of the biosensor fabricated for the determination of glucose. Therefore, the individual and cumulative effects of these variables were evaluated by using a statistical and mathematical technique known as CCD [28].

Table 3 presents the results obtained for the experimental design given in Table 2, which have been analyzed in terms of variance analysis (ANOVA) at 95% of confidence. $p < 0.05$ indicates if the random explanation is rejected there is less than 5% probability that this would be in error. The significance of the model was verified by Fisher's F test; the obtained F value of 15.13 at a low probability ($p < 0.0001$) shows significance of the model. Moreover, A ($p < 0.0001$), C ($p = 0.0218$), A^2 ($p < 0.0001$)), and B^2 ($p = 0.0006$) are significant model terms. By eliminating the non-significant parameters ($p < 0.05$), the mathematical model representing the actual relationship between the amperometric current response (nA) and the independent variables is expressed by the following second-order model:

$$Y = 1141.24 + 173.48[\text{c-MWCNT}] + 78.77[\text{GOx}] - 229.27[\text{c-MWCNT}]^2 - 129.03[\text{TiO}_2\text{NP}]^2$$

The lack-of-fit test is designed to evaluate whether this developed model is suitable to represent the experimental data, or whether another model should be used. The p value for lack-of-fit in Table 3 is 0.1182 ($p > 0.05$), indicating that the proposed model is suitable for the experimental data at the 95.0% confidence level. The obtained R^2 (0.9190) is satisfactory, showing that the electrode response is adequately fitted by the proposed model. A good correlation between experimental and predicted values was verified (Table 2).

Figure 1 shows the response surface plots of the amperometric currents as functions of c-MWCNT - TiO_2NP, c-MWCNT-GOx, and TiO_2NP-GOx. As can be seen from ANOVA, the quadratic terms of c-MWCNT and TiO_2NP were noticed to be significant, because β value in case of quadratic term was higher than the linear terms of c-MWCNT and TiO_2NP. In contrast, β value of the quadratic term was found to be lower than that of the linear term indicating that the linear term of GOx was significant. This showed that there was a curve relationship between the c-MWCNT or TiO_2NP amount and amperometric response current. Thus, initially, the amperometric current will increase with the increase in c-MWCNT or TiO_2NP amount and after reaching the maximum, the amperometric current decreases with the further increase of c-MWCNT or TiO_2NP amount (Fig. 1). However, amperometric response was almost linearly proportional to GOx amount (Fig. 1b, c). As a result, the obtained convex response surface depicted that the highest amperometric response was obtained when 24.1 mg mL^{-1} c-MWCNT, 22.2 mg mL^{-1} TiO_2NP, and 3.89 UμL^{-1} GOx were used for the modification of electrode surface. Decreasing the amounts of c-MWCNT, TiO_2NP, and GOx reduced the amperometric response, confirming that these three variables had significant influence on the electrode response. These conditions maximize the glucose response at the modified electrode and were therefore considered as the optimum ones for the electrode surface composition.

As generally commercially available enzymes are expensive and available in small quantities, a CCD with two factors (c-MWCNT and TiO_2NP) was performed taking the current registered for a 2.0×10^{-4} M solution of H_2O_2 as response and the results obtained from this design were compared with those obtained from 2^3 CCD. In 2^2 CCD, a total of 13 experiments were performed, including 4 factorial points, 4 axial points, and 5 central points. α value was used as 1.414 for ortagonal and rotatable design. Experimental factors and levels for this design are given in Electronic Supplementary Material (ESM) Table S1. ESM Tables S2 and S3 summarize

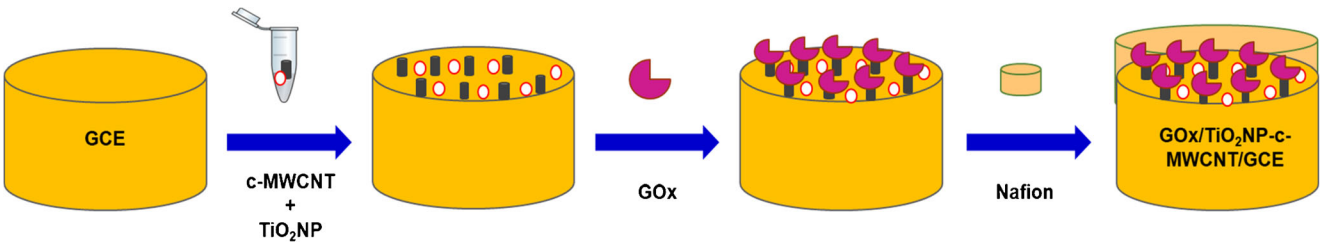

Scheme 1 The stepwise fabrication of the GOx/TiO_2-c-MWCNT-CT/GCE biosensor

Table 3 ANOVA with the data of the 2^3 CCD for the optimization of c-MWCNT, TiO_2NP and GOx amounts

Source	β	SS	df	MS	F value	P value	
Model	1141.24	1.66×10^6	9	1.85×10^5	15.13	< 0.0001	Significant
A	173.48	4.11×10^5	1	4.11×10^5	33.66	< 0.0001	Significant
B	58.77	4.72×10^4	1	4.72×10^4	3.86	0.0729	
C	78.77	8.47×10^4	1	8.47×10^4	6.94	0.0218	Significant
AB	79.25	5.02×10^4	1	5.02×10^4	4.12	0.0653	
AC	− 2.25	4.05×10^1	1	4.05×10^1	0.00	0.9550	
BC	− 39.75	1.26×10^4	1	1.26×10^4	1.04	0.3290	
A^2	− 229.27	8.14×10^5	1	8.14×10^5	66.70	< 0.0001	Significant
B^2	− 129.03	2.58×10^5	1	2.58×10^5	21.13	0.0006	Significant
C^2	− 38.88	2.34×10^4	1	2.34×10^4	1.92	0.1913	
Residual		1.47×10^5	12	1.22×10^4			
Lack of fit		9.59×10^4	5	1.92×10^4	2.65	0.1182	Not significant
Pure error		5.06×10^4	7	7.24×10^3			
Cor total		1.81×10^6	21				
$R^2 = 0.9190$							

SS, sum of squares; *df*, degrees of freedom; *MS*, mean squares; $F_{value} = MS_{factor}/MS_{error}$; P_{value}: probability level

the experimental and predicted amperometric response currents and the analysis of variance (ANOVA) for the regression model. In this design, analysis of the results showed that the quadratic terms of c-MWCNT and TiO_2NP and the linear term of c-MWCNT were significant factors at the 95.0% confidence level within the concentration ranges used in this application. These factors were also found to be significant in 2^3 CCD. ESM Fig. S1 shows the response surface plots of the amperometric current as a function of c-MWCNT and TiO_2NP amounts. It can be observed that a well-defined maximum is reached. From this optimization process, the following optimum values were obtained: 23.6 mg mL^{-1} c-MWCNT and 19.9 mg mL^{-1} TiO_2NP. These values were very close to the values obtained with 2^3 CCD. After the optimization of c-MWCNT and TiO_2NP amounts by 2^2 CCD design, the amount of GOx was optimized by varying the enzyme amount from 10 to 40 U. ESM Fig. S2 shows the effect of GOx loading on the biosensor response. The response current increased with increasing enzyme units, reaching a maximum between 30 and 40 U and afterward decreased. This enzyme unit was very close to the value (38.9 U) obtained from 2^3 CCD design. Considering the high cost of biological material, optimization of the other component amounts on an electrode surface by CCD and using conventional method for enzyme amount optimization can be an alternative approach for biosensor design.

To evaluate the effectiveness of CCD in the optimization of electrode surface composition, TiO_2NP and c-MWCNT amounts were also optimized by conventional one-factor-at-a-time method [42]. This method is applied by changing one factor at a time and keeping others fixed. First, c-MWCNT amount was varied between 0.5 and 3.0 mg mL^{-1} in 0.5 mg mL^{-1} increments and the best response was obtained with the electrode prepared with 1.5 mg mL^{-1} c-MWCNT (ESM Fig. S3). c-MWCNT amount was then fixed at this level. Next, the other factor TiO_2NP amount was changed between 1.0 and 3.0 mg mL^{-1} in 0.5 mg mL^{-1} increments until its best amount was found. The best current response was obtained with the electrode prepared with 1.0 mg mL^{-1} TiO_2NP and its amount was held constant at this value (ESM Fig. S4). In this study, the decrease in response currents after 1.5 mg mL^{-1} c-MWCNT and 1.0 mg mL^{-1} TiO_2NP limited the testing of higher amounts by the one-factor-at-a-time method. On the other hand, testing the same concentration range used in CCD approach by one-factor-at-a-time method involves many independent runs. Moreover, one-factor-at-a-time approach has some disadvantages such as impossibility in estimation of interactions among the factors and probability of optimum values missing [43, 44]. The MWCNT and TiO_2NP amounts obtained with one-factor-at-a-time method show that it is difficult to achieve the optimum amounts using this method for the optimization of electrode surface composition.

Surface morphology of modified electrodes

Scanning electron microscopy technique was used to investigate the effects of modification materials on the surface morphology of the electrodes. Figure 2 depicts the SEM images of (a) c-MWCNT-CT, (b) TiO_2-CT, (c) TiO_2-c-MWCNT-CT, and (d) GOx/TiO_2-c-MWCNT-CT modified GCE surfaces.

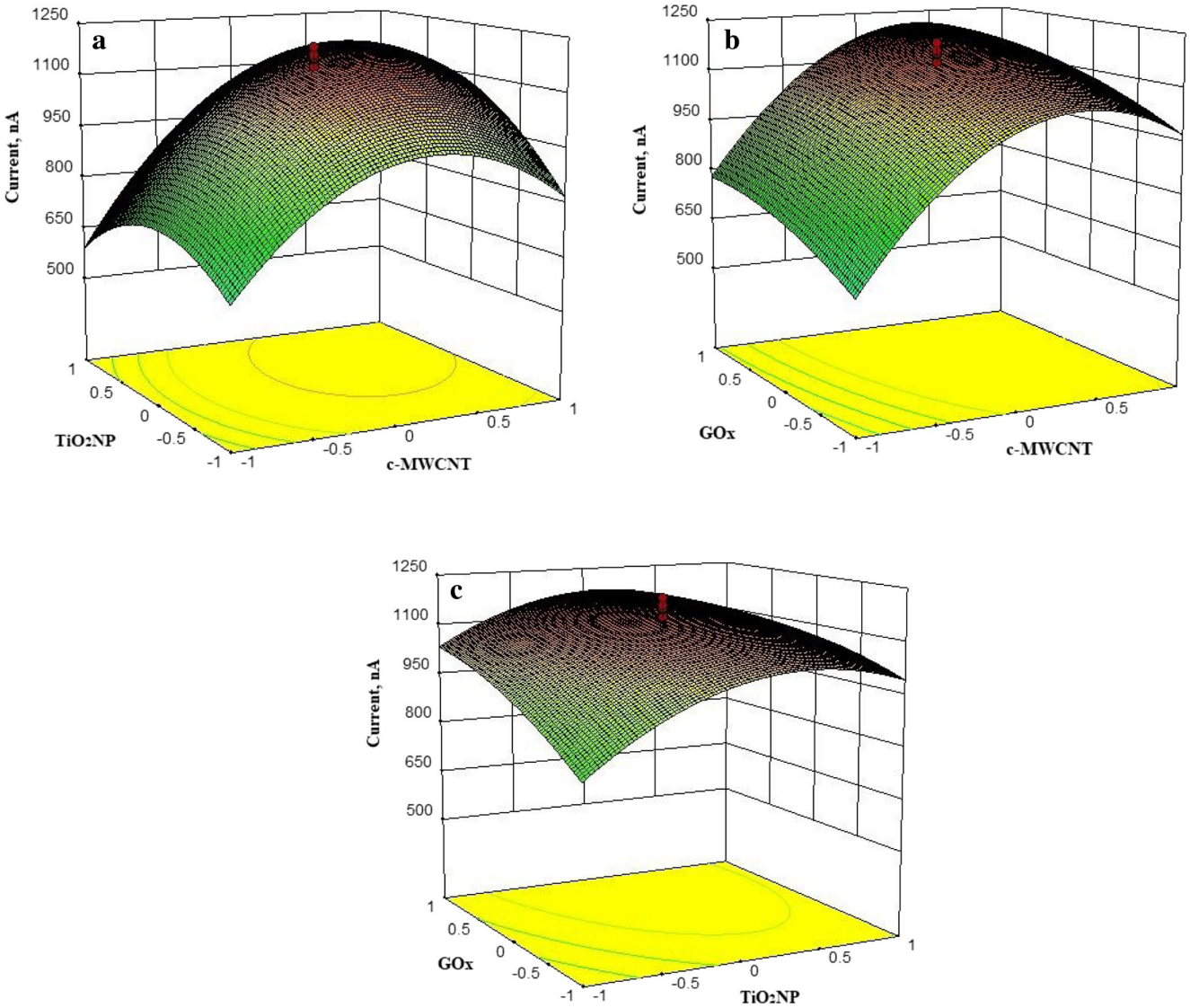

Fig. 1 Response surface plots of the amperometric current as a fuction of **a** c-MWCNT and TiO_2NP amounts, **b** c-MWCNT and GOx amounts, and **c** GOx and TiO_2NP amounts in the mixture used for the modification of GCE surface (in 0.025 M PBS containing 8.0×10^{-5} M glucose, at +0.70 V)

Figure 2a, b indicates that both c-MWCNT and TiO_2NP were homogenously dispersed in chitosan. Figure 2c confirms the co-existence of TiO_2NP and c-MWCNT and shows that these materials are well dispersed in chitosan. Moreover, TiO_2-c-MWCNT-CT modified GCE provides a porous and suitable platform for GOx immobilization. The change in the surface morphology of the GOx/TiO_2-c-MWCNT-CT/GCE (Fig. 2d) indicates that GOx enzyme was immobilized onto the TiO_2-c-MWCNT-CT/GCE. Elemental composition of the GOx/TiO_2-c-MWCNT-CT composite was studied by energy-dispersive X-ray test (EDX) (Fig. 2e). The Ti, P, Na, O, N, and C peaks in the spectra and the data given in the inset Table proved that the composite contained these elements. Taking into account the properties of c-MWCNT and TiO_2NP such as large surface area, nontoxicity, biocompability, and good chemical stability, it is expected that the TiO_2-c-MWCNT-CT matrix prepared in this study is desirable for biosensor applications.

CV and EIS characterization

The cyclic voltammograms of (a) TiO_2-CT/GCE and (b) TiO_2-c-MWCNT-CT/GCE are shown in Fig. 3a. The TiO_2-c-MWCNT-CT/GCE exhibits higher currents than TiO_2-CT/GCE implying the superior electron transfer properties associated with the carbon nanotubes [45]. EIS is an efficient method to study the interface features of surface modified electrodes. The diameter of the semicircle portion at higher frequencies of the Nyquist plot corresponds to the charge transfer resistance (R_{ct}), and this controls the electron transfer

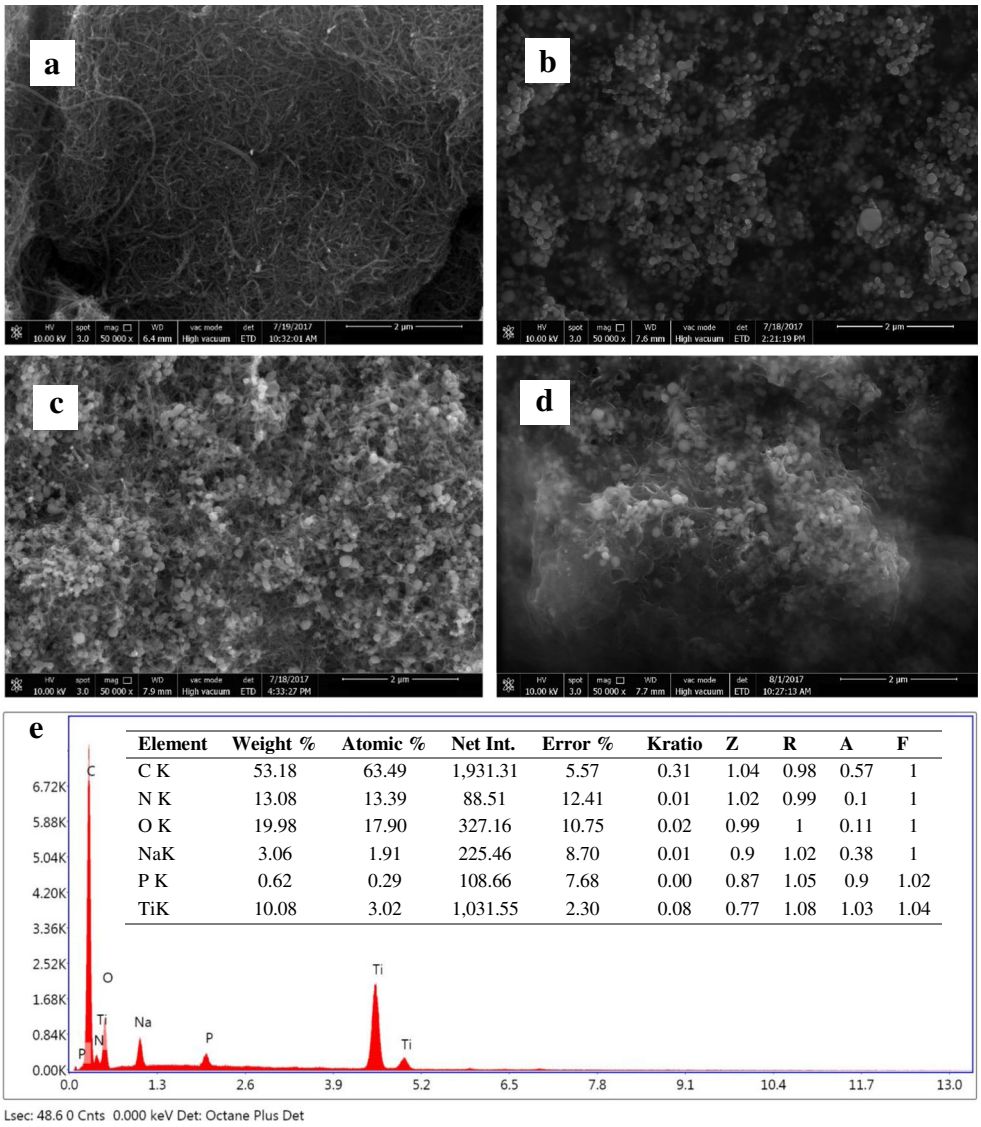

Fig. 2 SEM images of **a** c-MWCNT-CT/GCE, **b** TiO_2-CT/GCE, **c** TiO_2-c-MWCNT-CT/GCE, and **d** GOx/TiO_2-c-MWCNT-CT/GCE. (e) EDX spectra for the elements Ti, P, Na, O, N, and C (GOx/TiO_2-c-MWCNT-CT/GCE)

kinetics of the redox probe at the electrode interface. On the other hand, the linear part of the plot at lower frequencies corresponds to the diffusion process [46]. Figure 3b shows EIS of (a) TiO_2-CT/GCE and (b) TiO_2-c-MWCNT-CT/GCE in 0.1 M KCl containing 5.0 mM $K_3[Fe(CN)_6]$/$K_4[Fe(CN)_6]$ (1:1). It was observed that the R_{ct} of TiO_2-c-MWCNT-CT/GCE is lower than TiO_2-CT/GCE indicating that the TiO_2-c-MWCNT/CT composite decreases the

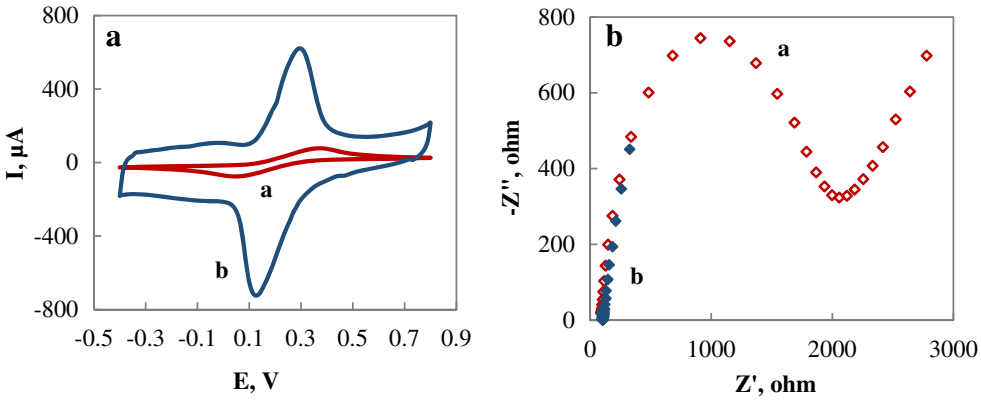

Fig. 3 **a** Cyclic voltammograms and **b** EIS of (a) TiO_2-CT/GCE and (b) TiO_2-c-MWCNT-CT/GCE in 0.1 M KCl containing 5.0 mM $K_3[Fe(CN)_6]$/$K_4[Fe(CN)_6]$

resistance of the electrode and possess higher electron transfer efficiency.

Optimization of experimental variables

The effects of experimental conditions on the response of the glucose biosensor constructed using the electrode composition optimized by means of 2^3 CCD were investigated.

The analytical performance of a biosensor is sensitive to the variation of buffer concentration in the test solution [47]. Therefore, the influence of buffer concentration on the response of the biosensor was studied by exposing it to 0.20 mM glucose in various phosphate buffer concentrations (0.025–0.10 M) at pH 8.0. The highest response was observed at 0.025 M and this concentration was chosen for further measurements. It can be suggested that high concentrations of phosphate may cause an inhibitory effect on the enzyme activity. Similar observation was reported in the literature [48].

The pH dependence of the biosensor response was tested at 0.20 mM glucose solution in the pH range 6.0–9.5 using 0.025 M PBS (Fig. 4). The biosensor displayed an optimum response at pH 8.0. The optimum pH for the free GOx in solution is around 5.5 [49]. The shift in optimum pH may be due to a change in enzyme conformation when immobilized at the electrode surface [50].

Enzymes are susceptible to thermal denaturation [51, 52]. Thus, thermal stability is an important parameter in practical use of the biosensors. The thermal stability of the GOx/TiO_2-c-MWCNT-CT/GCE biosensor was investigated between 25 and 50 °C in the presence of 0.20 mM glucose. The response of the biosensor increased with the increase in the working temperatures from 25 to 40 °C (data not shown). The response decreased at temperatures higher than 40 °C which probably was due to the partial denaturation of the enzyme [51]. Although best current response was obtained at 40 °C, glucose measurements were performed at room temperature in order to simplify the experimental procedures.

Performance parameters

The electrode surface compositions optimized by one-factor-at-a-time method, 2^2 CCD and 2^3 CCD were used in the fabrication of glucose biosensors and the analytical characteristics of these biosensors were compared in terms of detection limit, linear working range and sensitivity. Figure 5a, b, c depicts the calibration curves and current–time plots (inset) for the GOx/TiO_2-c-MWCNT-CT/GCE biosensors constructed using the electrode compositions optimized by means of one-factor-at-a-time method, 2^2 CCD and 2^3 CCD, respectively. The calibration curves were obtained under optimal experimental conditions with successive step changes of glucose concentration. The biosensor constructed using the optimum values obtained from one-factor-at-a-time method showed a

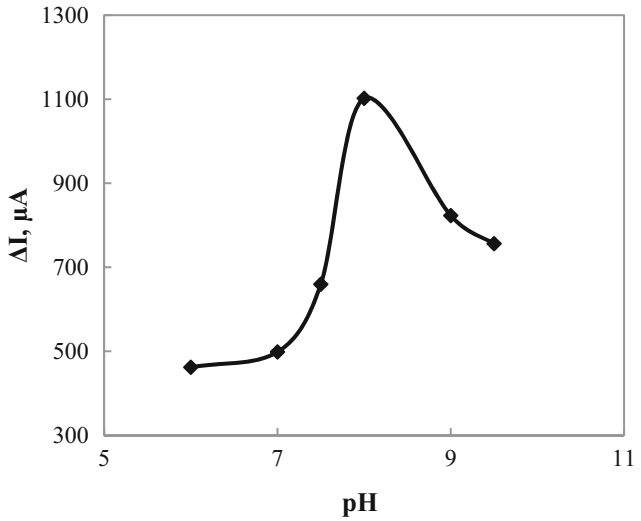

Fig. 4 Effect of pH on the response of GOx/TiO_2-c-MWCNT-CT/GCE (in 0.025 M PBS at + 0.70 V)

linear relationship with the concentration of glucose from 2.0×10^{-5} to 6.8×10^{-4} M (Fig. 5a) with a sensitivity of 1.75 μA mM^{-1} and detection limit of 8.3×10^{-6} M. The low sensitivity obtained with this biosensor was probably due to the low amounts of c-MWCNT and TiO_2NP used for electrode modification. The linear working range of the glucose biosensor constructed using the optimum values obtained from 2^2 CCD was 2.0×10^{-5} to 2.3×10^{-3} M with a correlation coefficient of 0.9967 (Fig. 5b). The sensitivity and detection limit of this biosensor were found as 9.36 μA mM^{-1} and 3.2×10^{-6} M, respectively. On the other hand, GOx/TiO_2-c-MWCNT-CT/GCE constructed using the electrode composition optimized by means of 2^3 CCD exhibited a linear range between 2.0×10^{-5} and 1.9×10^{-3} M with a correlation coefficient of 0.9941 and a sensitivity of 11.96 μA mM^{-1} (168.5 μA mM^{-1} cm^{-2}) (Fig. 5c). The detection limit of the biosensor was calculated as 2.1×10^{-6} M at a signal/noise ratio of 3. The sensitivity, detection limit, and linear range of the biosensors constructed using the optimum values obtained from 2^2 CCD and 2^3 CCD were similar. This result indicates that optimization of the TiO_2NP and c-MWCNT amounts by CCD and optimization of enzyme amount by the conventional method can also be used for biosensor design especially in case of expensive enzymes.

The results show that the glucose biosensor constructed using the optimum values obtained from 2^3 CCD showed the highest sensitivity and lowest detection limit. Therefore, other analytical performance characteristics such as substrate selectivity and operational stability were investigated only for this biosensor. The biosensor achieved 95% of steady current within 20 s which is lower than that reported for glucose biosensors based on AgNPs modified TiO_2 nanotube arrays [53] but comparable to TiO_2NP/Nafion modified contact lens [54]. The sensitivity of the biosensor (168.5 μA mM^{-1} cm^{-2})

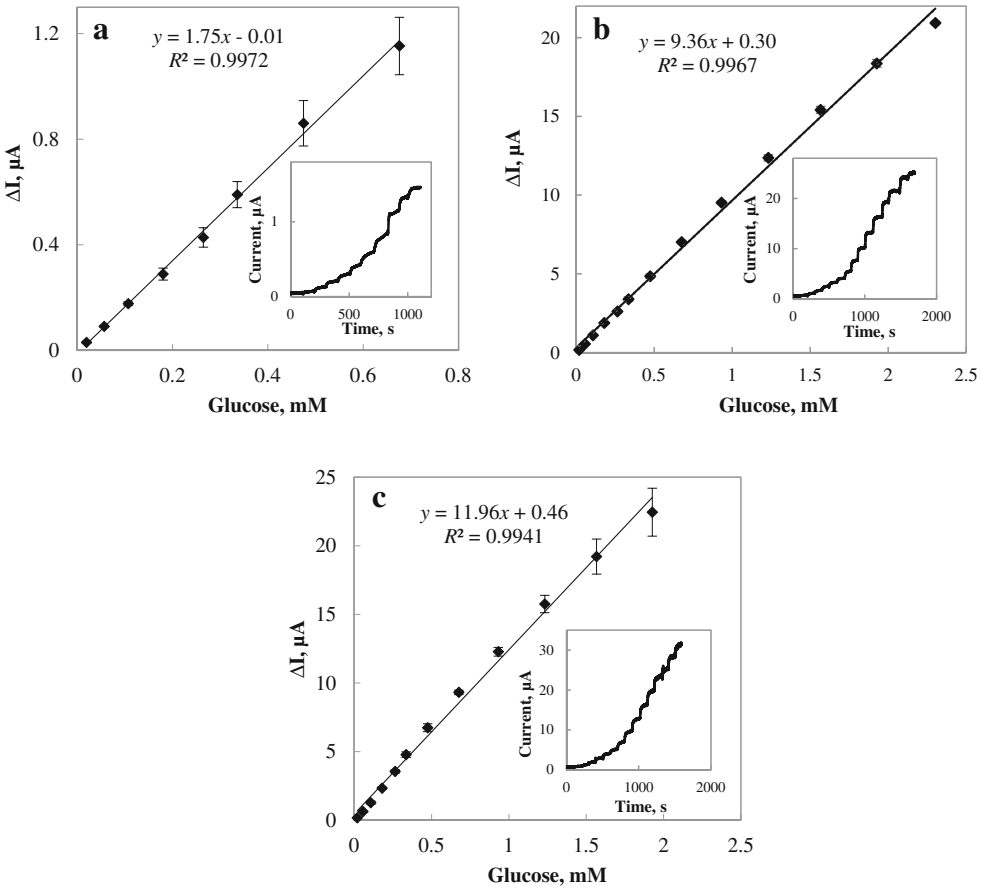

Fig. 5 Calibration curves and current–time plots (inset) for the GOx/TiO_2-c-MWCNT-CT/GCE biosensors constructed using the electrode compositions optimized by means of **a** one-factor-at-a-time method, **b** 2^2 CCD, and **c** 2^3 CCD (0.025 M PBS at +0.70 V error bars show the standard deviation of three measurements)

is higher than the sensitivities obtained with the glucose biosensors based on TiO_2 nanotube arrays modified with graphene and Pt nanoparticles [55], TiO_2 nanofibers modified Pt electrodes [56], Pt/carbon nanotubes/TiO_2NTs modified Ti electrodes [57], Pt-Au/TiO_2 nanotube arrays modified Ti electrodes [58], TiO_2NP and graphene modified GCE [59] and TiO_2NP/graphene/NiO modified GCE [60]. Moreover, the linear range of the biosensor is superior to that of the previously reported glucose biosensors based on TiO_2NP and graphene modified GCE [59] and TiO_2NP/graphene/NiO modified GCE [60]. This improved performance can be attributed to the increase of electroactive surface area and the synergistic effect of TiO_2NP and MWCNT. The apparent Michaelis–Menten constant (K_M^{app}) can be used to evaluate the enzymatic activity of the immobilized GOx. In our study, K_M^{app} value, calculated according to the Lineweaver–Burk equation [61] was found to be 5.9 mM for the glucose biosensor. The K_M^{app} values reported for GOx in multilayer films composed of MWCNT and gold nanoparticles [62] and GOx in titania sol–gel membrane [54] were 14.9 mM and 11 mM, respectively. The smaller K_M^{app} value indicates that the presented biosensor exhibits a higher affinity for glucose than the above biosensors.

High selectivity is very important for glucose biosensors since easily oxidized substances co-exist with glucose in human serum. For the determination of substrate, selectivity of the glucose biosensor various substances such as urea, glucose, ascorbic acid, uric acid, and NaCl was examined at +0.70 V vs. Ag/AgCl in pH 8.0, 0.025 M PBS. The normal physiological level of glucose is 30–50 times higher than those of the interfering species such as ascorbic acid and uric acid [63]. Therefore, the effect of these substances was investigated at the following concentrations: urea (0.02 mM), glucose (1.0 mM), ascorbic acid (0.02 mM), uric acid, (0.02 mM) and NaCl (0.02 mM). Addition of urea and NaCl did not produce observable interference in the biosensor response. Compared with the response current change of biosensor to glucose, the relative response current change was approximately 6% for ascorbic acid and 7% for uric acid. These results indicate that the presented glucose biosensor has high selectivity.

Operational stability of the biosensor was studied by running sequential measurements in the presence of 0.20 mM glucose. Relative standard deviation (RSD%) of the biosensor response was lower than 5% for 50 successive measurements indicating the biosensor exhibits a good operation stability. The good operational stability of the biosensor can be attributed to the following aspect: The TiO_2-c-MWCNT-CT composite provided a biocompatible microenvironment for retaining the activity of GOx. Such good operational stability

Table 4 Characteristics of various TiO_2 nanomaterial based amperometric glucose biosensors reported in recent years

Electrode Modification	Working potential (V)	Sensitivity	Detection limit	Linear range	Response time (s)	Ref.
GOx/Ag/TiO_2NTAs/Pt electrode	+ 0.70	0.39 μA mM^{-1} cm^{-2}	0.1 mM	0.1–4 mM	40	[53]
GOD/titania sol–gel film/Nafion/ PET/contact lens	+ 0.40	240 μA mM^{-1} cm^{-2}	0.01 mM	0.1–0.6 mM	< 20	[54]
GOx/PtNPs/GR/TiO_2NTAs	+ 0.70	0.94 μA mM^{-1} cm^{-2}	0.1 mM	0.1–8 mM	–	[55]
Chit/GOx/TiO_2 nanofibers/Pt electrode	+ 0.60	9.25 μA mM^{-1} cm^{-2}	0.01 μM	0.01–6.98 mM	10	[56]
GOx/ Pt nanoparticle-decorated CNT/TiO_2NT electrode	+ 0.40	0.24 μA mM^{-1} cm^{-2}	5.7 μM	0.006–1.5 mM	3	[57]
GOx/Pt-Au/TiO_x NT	− 0.20	0.08366 μA mM^{-1}	0.1 mM	0–1.8 mM	3	[58]
GOD/TiO_2NPs/GR/GCE	− 0.60	6.2 μA mM^{-1} cm^{-2}		0–8 mM		[59]
GOD/NiO/TiO_2-GR/GCE	− 0.30	4.129 μA mM^{-1}	1.2 μM	1–12 mM	3	[60]
GOD/PDDA-Au/PB/TiO_2-MWCNTs-Chit/GCE	− 0.10	–	0.1 μM	6 μM −1.2 mM		[19]
GOD/MAA/AuNPs/TiO_2NT/Ti electrode	− 0.25	–	0.31 mM	0.40–8.00 mM	10	[64]
TNT-GNP|([Demim]Br|Nafion| GOD|GCE	–	5.1 mA mM^{-1}		0.01–1.2 mM	–	[65]
Pt-DENs/TNTs/GOx/GCE	− 0.35	43.6 μA mM^{-1} cm^{-2}	1 μM	2 μM - 12 mM	3	[66]
GOx/n-TiO_2/ polyaniline/activecarbon/GCE	− 0.45	6.31 μA mM^{-1} cm^{-2}	18 μM	0.02–6.0 mM	10	[67]
PANI-TNTs|([Demim]Br|Nafion| GOD|GCE	–	11.4 μA mM^{-1}	0.5 μM	10–2500 μM		[17]
GOx/TiO_2-c-MWCNT-CT/GCE	+ 0.70	11.9 μA mM^{-1} (168.5 μA mM^{-1} cm^{-2})	2.1 μM	0.02–1.9 mM	< 20	This work

Ag silver nanoparticles, *TiO_2NTAs* TiO_2 nanotube arrays, *GOD* glucose oxidase, *GR* graphene, *PtNPs* platinum nanoparticles, *PET* polyethylene terephthalate polymer, *Chit* chitosan, *CNT* carbon nanotube, *TiO_2NT* titanium nanotubes, *Pt-Au/TiO_x NT* gold–platinum nanoparticle-decorated titania nanotubular electrode, *NiO* nickel oxide nanoparticles, *PB* Prussian blue, *PDDA* poly (diallyldimethylammonium chloride), *Au* gold nanoparticles, *MAA* mercaptoacetic acid, *TNT* titanate nanotubes, *GNP* gold nanoparticles, *PANI* polyaniline, *TNTs* titanium nanotubes, *Pt-DENs* poly (amidoamine) dendrimers encapsulated platinum nanoparticles, *n-TiO_2* nanometer-sized TiO_2

is essential for any commercial biosensor device. The relative standard deviation (RSD, $n = 3$) of the biosensor response was 3.4%, with different electrodes prepared following the same procedure, verifying the good reproducibility of the biosensor.

The performance characteristics of the presented glucose biosensor were compared with other TiO_2 nanomaterial-based glucose biosensors in Table 4. It can be concluded that the presented biosensor possesses excellent performance in terms of high sensitivity, low detection limit, anti-interference ability to common electroactive species found in biological samples and good operational stability.

Real sample analysis

The influence of common interfering compounds on biosensor response should be evaluated prior to the analysis of real samples to ensure its applicability. In our study, the tested substances did not interfere significantly with the biosensor response. Therefore, the resulting biosensor was used for glucose assay for human serum samples and the results were compared with those obtained by the spectrophotometric method. Standard addition method was used for the determination of glucose in serum samples. After the current response was recorded in a 5.0 mL of 0.025 M PBS containing 10 μL of serum sample, five 0.01 M glucose solutions of 10 μL were successively added to the electrochemical cell for standard addition determination. The results obtained with the biosensor showed a good correlation ($y = 0.9124x + 6.5445$, $R^2 = 0.9798$) with those obtained by the reference method (Table 5). The accuracy of the method was also checked by *t* test. The *t* value is 2.39 for the biosensor at 95% confidence level, for which t_{critic} is 2.57. It can be concluded that there is no difference between the results of two methods at a

Table 5 Results obtained from the analysis of the serum samples by the GOx/TiO_2-c-MWCNT-CT/GCE and spectrophotometric method (reference)

	Glucose mg mL^{-1}	
Sample	Biosensor[a] method	Spectrophotometric method
1	77.8 ± 0.5	77
2	83.4 ± 0.2	83
3	94.0 ± 0.6	93
4	88.6 ± 0.7	88
5	98.2 ± 4.9	94
6	101.3 ± 0.5	100

[a] Average of three measurements

confidence level of 95%. As a result, the developed glucose biosensor can be useful for the efficient determination of glucose present in serum samples and provides a good alternative for the reference method, especially in respect to sensitivity, selectivity, stability and rapid response. Moreover, the biosensor method presented in this study did not require pretreatment of the samples.

Conclusion

We have demonstrated the feasibility of using 2^3 CCD for the optimization of electrode surface composition (for c-MWCNT, TiO_2 and GOx amounts) to fabricate an amperometric glucose biosensor. The resulting biosensor showed high sensitivity and selectivity, good operational stability and successfully applied to the analysis of glucose in serum samples which confirmed the effectiveness of CCD in the optimization of electrode surface composition. The results obtained with the presented biosensor were compared with those obtained with the glucose biosensors constructed using the electrode compositions optimized by 2^2 CCD (for c-MWCNT and TiO_2NP amounts) and conventional one-at-a-time approach. The analytical performance of the biosensors constructed using the optimum values obtained from 2^2 CCD and 2^3 CCD were found to be similar. Considering the high cost of enzymes, optimization of the c-MWCNT and TiO_2NP amounts by 2^2 CCD and using conventional method for the optimization of enzyme amount might be a good alternative for biosensor design. On the other hand, the glucose biosensor optimized by means of a one-factor-at-a-time method showed the worst analytical performance. The tested range of c-MWCNT and TiO_2NP amounts in one-factor-at-a-time method was very narrow and the optimized amounts did not reflect the real optimum values. This result indicates that the range used for the optimization of the modification materials in one-factor-at-a-time method should be well defined. It can be concluded that CCD could be an effective tool to determine optimum electrode surface composition in biosensor fabrication. In comparison with the time-consuming one factor-at-a-time method, CCD gives the most information with the fewest experimental runs. Moreover, CDD facilitates an understanding of the influence of the factors tested and the interactions between these factors on biosensor response. Therefore, the approach is promising for the development of other biosensors. Works on this aspect are under way in our laboratory.

Acknowledgments Financial support of The Scientific and Technological Research Council of Turkey (Project No: 116Z159) for Design-Expert software package is gratefully acknowledged.

Compliance with ethical standards

Human serum samples used in this study were collected from healthy volunteers. This work was performed with the written informed consent of the volunteers. The collected samples were anonymized before the study. The studies have been approved by Clinical Research Ethics Committee of the Faculty of Medicine, Ankara University and have been performed in accordance with ethical standards.

Conflict of interest The authors declare that they have no conflict of interest.

References

1. Mousty C. Biosensing applications of clay-modified electrodes: a review. Anal Bioanal Chem. 2010;396(1):315–25.
2. Song Y, Su D, Shen Y, Liu H, Wang L. Design and preparation of open circuit potential biosensor for in vitro and in vivo glucose monitoring. Anal Bioanal Chem. 2017;409(1):161–8.
3. Lai J, Yi Y, Zhu P, Shen J, Wu K, Zhang L, et al. Polyaniline-based glucose biosensor: a review. J Electroanal Chem. 2016;782:138–53.
4. Zhu C, Yang G, Li H, Du D, Lin Y. Electrochemical sensors and biosensors based on nanomaterials and nanostructures. Anal Chem. 2014;87(1):230–49.
5. Holzinger M, Le Goff A, Cosnier S. Nanomaterials for biosensing applications: a review. Front Chem. 2014;2(63):1–10.
6. Yang C, Denno ME, Pyakurel P, Venton BJ. Recent trends in carbon nanomaterial-based electrochemical sensors for biomolecules: a review. Anal Chim Acta. 2015;887:17–37.
7. Dalkıran B, Erden PE, Kılıç E. Amperometric biosensors based on carboxylated multiwalled carbon nanotubes-metal oxide nanoparticles-7, 7, 8, 8-tetracyanoquinodimethane composite for the determination of xanthine. Talanta. 2017;167:286–95.
8. Mallakpour S, Khadem E. Carbon nanotube–metal oxide nanocomposites: fabrication, properties and applications. Chem Eng J. 2016;302:344–67.
9. Panigrahi AK, Singh V, Singh SG. A multi-walled carbon nanotube–zinc oxide nanofiber based flexible chemiresistive biosensor for malaria biomarker detection. Analyst. 2017;142(12):2128–35.
10. Dalkıran B, Erden PE, Kılıç E. Electrochemical biosensing of galactose based on carbon materials: graphene versus multi-walled carbon nanotubes. Anal Bioanal Chem. 2016;408(16):4329–39.
11. Kaçar C, Erden PE, Kılıç E. Amperometric l-lysine biosensor based on carboxylated multiwalled carbon nanotubes-SnO_2 nanoparticles-graphene composite. Appl Surf Sci. 2017;419:916–23.
12. Lee J, Morita M, Takemura K, Park EY. A multi-functional gold/iron-oxide nanoparticle-CNT hybrid nanomaterial as virus DNA sensing platform. Biosens Bioelectron. 2018;102:425–31.
13. Palanisamy S, Cheemalapati S, Chen SM. Highly sensitive and selective hydrogen peroxide biosensor based on hemoglobin immobilized at multiwalled carbon nanotubes-zinc oxide composite electrode. Anal Bioanal Chem. 2012;429(2):108–15.
14. Periasamy AP, Yang S, Chen SM. Preparation and characterization of bismuth oxide nanoparticles-multiwalled carbon nanotube composite for the development of horseradish peroxidase based H_2O_2 biosensor. Talanta. 2011;87:15–23.
15. Liu X, Yan R, Zhu J, Huo X, Wang X. Development of a photoelectrochemical lactic dehydrogenase biosensor using multi-wall carbon nanotube-TiO_2 nanoparticle composite as coenzyme regeneration tool. Electrochim Acta. 2015;173:260–7.

16. Sun W, Guo Y, Ju X, Zhang Y, Wang X, Sun Z. Direct electrochemistry of hemoglobin on graphene and titanium dioxide nanorods composite modified electrode and its electrocatalysis. Biosens Bioelectron. 2013;42:207–13.
17. Zhu J, Liu X, Wang X, Huo X, Yan R. Preparation of polyaniline–TiO_2 nanotube composite for the development of electrochemical biosensors. Sensors Actuators B Chem. 2015;221:450–7.
18. Bai J, Zhou B. Titanium dioxide nanomaterials for sensor applications. Chem Rev. 2014;114(19):10131–76.
19. Zhang M, Yuan R, Chai Y, Li W, Zhong H, Wang C. Glucose biosensor based on titanium dioxide-multiwall carbon nanotubes-chitosan composite and functionalized gold nanoparticles. Bioprocess Biosyst Eng. 2011;34(9):1143–50.
20. Terracciano M, Galstyan V, Rea I, Casalino M, De Stefano L, Sbervegleri G. Chemical modification of TiO_2 nanotube arrays for label-free optical biosensing applications. Appl Surf Sci. 2017;419:235–40.
21. Shu J, Qiu Z, Lv S, Zhang K, Tang D. Plasmonic enhancement coupling with defect-engineered TiO_2–x: a mode for sensitive Photoelectrochemical biosensing. Anal Chem. 2018;90(4):2425–9.
22. Cai G, Yu Z, Ren R, Tang D. Exciton–Plasmon interaction between AuNPs/graphene nanohybrids and CdS quantum dots/TiO_2 for photoelectrochemical aptasensing of prostate-specific antigen. ACS Sens. 2018;3(3):632–9.
23. Qiu Z, Shu J, Tang D. Near-infrared-to-ultraviolet light-mediated photoelectrochemical aptasensing platform for cancer biomarker based on core–shell $NaYF_4$: Yb, Tm@ TiO_2 upconversion microrods. Anal Chem. 2017;90(1):1021–8.
24. Liu X, Yan R, Zhu J, Zhang J, Liu X. Growing TiO_2 nanotubes on graphene nanoplatelets and applying the nanonanocomposite as scaffold of electrochemical tyrosinase biosensor. Sensors Actuators B Chem. 2015;209:328–35.
25. Bardajee GR, Azimi S, Sharifi MBS. Application of central composite design for methyl red dispersive solid phase extraction based on silver nanocomposite hydrogel: microwave assisted synthesis. Microchem J. 2017;133:358–69.
26. Dastkhoon M, Ghaedi M, Asfaram A, Arabi M, Ostovan A, Goudarzi A. Cu@ SnS/SnO_2 nanoparticles as novel sorbent for dispersive micro solid phase extraction of atorvastatin in human plasma and urine samples by high-performance liquid chromatography with UV detection: application of central composite design (CCD). Ultrason Sonochem. 2017;36:42–9.
27. Alonso-Lomillo MA, Ruiz JG, Pascual FJM. Biosensor based on platinum chips for glucose determination. Anal Chim Acta. 2005;547(2):209–14.
28. Situmorang M, Hibbert DB, Gooding JJ. An experimental design study of interferences of clinical relevance of a polytyramine immobilized-enzyme biosensor. Electroanalysis. 2000;12(2):111–9.
29. Calvo MEB, Renedo OD, Martínez MJA. Optimization of the experimental parameters in the determination of lamotrigine by adsorptive stripping voltammetry. Anal Chim Acta. 2005;549(1–2):74–80.
30. Dashtian K, Zare-Dorabei R. Synthesis and characterization of functionalized mesoprous SBA-15 decorated with Fe_3O_4 nanoparticles for removal of Ce (III) ions from aqueous solution: ICP–OES detection and central composite design optimization. J Colloid Interface Sci. 2017;494:114–23.
31. Alonso-Lomillo MA, Domínguez-Renedo O, Hernández-Martín A, Arcos-Martínez MJ. Horseradish peroxidase covalent grafting onto screen-printed carbon electrodes for levetiracetam chronoamperometric determination. Anal Biochem. 2009;395(1):86–90.
32. Talat M, Singh AK, Srivastava ON. Optimization of process variables by central composite design for the immobilization of urease enzyme on functionalized gold nanoparticles for various applications. Bioprocess Biosyst Eng. 2011;34(6):647–57.
33. Asturias-Arribas L, Alonso-Lomillo MA, Domínguez-Renedo O, Arcos-Martínez MJ. CYP450 biosensors based on screen-printed carbon electrodes for the determination of cocaine. Anal Chim Acta. 2011;685(1):15–20.
34. Alonso-Lomillo MA, Domínguez-Renedo O, Ferreira-Gonçalves L, Arcos-Martínez MJ. Sensitive enzyme-biosensor based on screen-printed electrodes for ochratoxin A. Biosens Bioelectron. 2010;25(6):1333–7.
35. Retama JR, López MSP, Pérez JH, Cabanillas GF, López-Cabarcos E, López-Ruiz B. Biosensors based on acrylic microgels: a comparative study of immobilized glucose oxidase and tyrosinase. Biosens Bioelectron. 2005;20(11):2268–75.
36. Ivanov Y, Marinov I, Gabrovska K, Dimcheva N, Godjevargova T. Amperometric biosensor based on a site-specific immobilization of acetylcholinesterase via affinity bonds on a nanostructured polymer membrane with integrated multiwall carbon nanotubes. J Mol Catal B Enzym. 2010;63(3):141–8.
37. Martins SAM, Prazeres DMF, Fonseca LP, Monteiro GA. Application of central composite design for DNA hybridization onto magnetic microparticles. Anal Biochem. 2009;391(1):17–23.
38. Del Torno-de Román L, Alonso-Lomillo MA, Domínguez-Renedo O, Arcos-Martínez MJ. Gluconic acid determination in wine by electrochemical biosensing. Sensors Actuators B Chem. 2013;176:858–62.
39. Zhu Z, Garcia-Gancedo L, Flewitt AJ, Xie H, Moussy F, Milne WI. A critical review of glucose biosensors based on carbon nanomaterials: carbon nanotubes and graphene. Sensors. 2012;12(5):5996–6022.
40. Chen C, Xie Q, Yang D, Xiao H, Fu Y, Tan Y, et al. Recent advances in electrochemical glucose biosensors: a review. RSC Adv. 2013;3(14):4473–91.
41. Wang Y, Liu L, Li M, Xu S, Gao F. Multifunctional carbon nanotubes for direct electrochemistry of glucose oxidase and glucose bioassay. Biosens Bioelectron. 2011;30(1):107–11.
42. Banik RM, Pandey DK. Optimizing conditions for oleanolic acid extraction from Lantana camara roots using response surface methodology. Ind Crop Prod. 2008;27(3):241–8.
43. Nasirizadeh N, Dehghanizadeh H, Yazdanshenas ME, Moghadam MR, Karimi A. Optimization of wool dyeing with rutin as natural dye by central composite design method. Ind Crop Prod. 2012;40:361–6.
44. Czitrom V. One-factor-at-a-time versus designed experiments. Am Stat. 1999;53(2):126–31.
45. Thandavan K, Gandhi S, Nesakumar N, Sethuraman S, Rayappan JBB, Krishnan UM. Hydrogen peroxide biosensor utilizing a hybrid nano-interface of iron oxide nanoparticles and carbon nanotubes to assess the quality of milk. Sensors Actuators B Chem. 2015;215:166–73.
46. Lisdat F, Schäfer D. The use of electrochemical impedance spectroscopy for biosensing. Anal Bioanal Chem. 2008;391(5):1555–67.
47. Zhang Y, Wen G, Zhou Y, Shuang S, Dong C, Choi MM. Development and analytical application of an uric acid biosensor using an uricase-immobilized eggshell membrane. Biosens Bioelectron. 2007;22(8):1791–7.
48. Crouch E, Cowell DC, Hoskins S, Pittson RW, Hart JP. A novel, disposable, screen-printed amperometric biosensor for glucose in serum fabricated using a water-based carbon ink. Biosens Bioelectron. 2005;21(5):712–8.
49. Bright HJ, Appleby M. The pH dependence of the individual steps in the glucose oxidase reaction. J Biol Chem. 1969;244(13):3625–34.

50. Rodrigues RC, Ortiz C, Berenguer-Murcia Á, Torres R, Fernández-Lafuente R. Modifying enzyme activity and selectivity by immobilization. Chem Soc Rev. 2013;42(15):6290–307.
51. Wang YT, Yu L, Wang J, Lou L, Du WJ, Zhu ZQ, et al. A novel L-lactate sensor based on enzyme electrode modified with ZnO nanoparticles and multiwall carbon nanotubes. J Electroanal Chem. 2011;661(1):8–12.
52. Weetal HH. Enzymatic gallic acid esterification. Biotechnol Bioeng. 1985;27(2):124–7.
53. Feng C, Xu G, Liu H, Lv J, Zheng Z, Wu Y. Glucose biosensors based on Ag nanoparticles modified TiO_2 nanotube arrays. J Solid State Electrochem. 2014;18(1):163–71.
54. Yao H, Shum AJ, Cowan M, Lähdesmäki I, Parviz BA. A contact lens with embedded sensor for monitoring tear glucose level. Biosens Bioelectron. 2011;26(7):3290–6.
55. Feng C, Xu G, Liu H, Lv J, Zheng Z, Wu Y. Facile fabrication of Pt/graphene/TiO_2 NTAs based enzyme sensor for glucose detection. J Electrochem Soc. 2014;161(1):B1–8.
56. Tang H, Yan F, Tai Q, Chan HL. The improvement of glucose bioelectrocatalytic properties of platinum electrodes modified with electrospun TiO_2 nanofibers. Biosens Bioelectron. 2010;25(7):1646–51.
57. Pang X, He D, Luo S, Cai Q. An amperometric glucose biosensor fabricated with Pt nanoparticle-decorated carbon nanotubes/TiO_2 nanotube arrays composite. Sensors Actuators B Chem. 2009;137(1):134–8.
58. Kang Q, Yang L, Cai Q. An electro-catalytic biosensor fabricated with Pt–Au nanoparticle-decorated titania nanotube array. Bioelectrochemistry. 2008;74(1):62–5.
59. Jang HD, Kim SK, Chang H, Roh KM, Choi JW, Huang J. A glucose biosensor based on TiO_2–graphene composite. Biosens Bioelectron. 2012;38(1):184–8.
60. Xu CX, Huang KJ, Chen XM, Xiong XQ. Direct electrochemistry of glucose oxidase immobilized on TiO_2–graphene/nickel oxide nanocomposite film and its application. J Solid State Electrochem. 2012;16(12):3747–52.
61. Kamin RA, Wilson GS. Rotating ring-disk enzyme electrode for biocatalysis kinetic studies and characterization of the immobilized enzyme layer. Anal Chem. 1980;52(8):1198–205.
62. Wu BY, Hou SH, Yin F, Zhao ZX, Wang YY, Wang XS, et al. Amperometric glucose biosensor based on multilayer films via layer-by-layer self-assembly of multi-wall carbon nanotubes, gold nanoparticles and glucose oxidase on the Pt electrode. Biosens Bioelectron. 2007;22(12):2854–60.
63. Dayakar T, Rao KV, Bikshalu K, Rajendar V, Park SH. Novel synthesis and structural analysis of zinc oxide nanoparticles for the non enzymatic glucose biosensor. Mater Sci Eng C. 2017;75:1472–9.
64. Zhang Z, Xie Y, Liu Z, Rong F, Wang Y, Fu D. Covalently immobilized biosensor based on gold nanoparticles modified TiO_2 nanotube arrays. J Electroanal Chem. 2011;650:241–7.
65. Zhao R, Liu X, Zhang J, Zhu J, Wong DKY. Enhancing direct electron transfer of glucose oxidase using a gold nanoparticle titanate nanotube nanocomposite on a biosensor. Electrochim Acta. 2015;163:64–70.
66. Han X, Zhu Y, Yang X, Li C. Electrocatalytic activity of Pt doped TiO_2 nanotubes catalysts for glucose determination. J Alloys Compd. 2010;500:247–51.
67. Tang W, Li L, Zeng X. A glucose biosensor based on the synergistic action of nanometer-sized TiO_2 and polyaniline. Talanta. 2015;131:417–23.